Supplementary Information (SI) for Journal of Materials Chemistry A.
This journal is © The Royal Society of Chemistry 2025

Supporting Information

Self-Healing and Stretchable Tetrameric PVA-CNF-PVP-IL Complex Ionogel with High-Performance Ionic Thermoelectric Properties

*Xiaolin Wang, Yifang Jin, Hang Fu, Lianji Zhang, Patrick C. Lee, Chengjin An**

Experimentation Section

Materials: poly(vinylpyrrolidone) (PVP), sulfoxide (DMSO), Methylene blue CNF purchased from InnoChem. Poly(vinyl alcohol) (PVA) and carboxylated cellulose nanofibers (CNF) were purchased from Macklin. 1-ethyl-3-methylimidazolium dicyanamide (EMIM:DCA) was obtained from Lanzhou Institute of Chemical Physics, China.

Preparation of the ionogels: Aqueous solutions of PVA, CNF, and PVP were gradually mixed together to obtain a viscous but homogeneous solution, after which EMIM:DCA was added and mixed well. The obtained solution was poured into a Teflon or silicone mold and dried in an oven at 50 °C for 15 h to remove all solvent residues and obtain a free-standing ionogel film, which was stabilized for 12 h and then peeled off from the mold to obtain a transparent, healing ionogel.

Characterizations of thermoelectric properties: The ionic conductivity of the ionogels was determined by electrochemical AC impedance spectroscopy (EIS) using an electrochemical workstation (CHI660E) with a voltage amplitude of 10 mV and a frequency ranging from 100 kHz to 0.1 Hz. The ionogel films were sandwiched

between two Pt sheets. The ionic resistance was obtained by extrapolating the curve to the abscissa based on the equivalent shown in **Scheme S1**: The ionic conductivity was calculated using the following equation:

$$\sigma_{ion} = \frac{1}{RA}L \quad \text{(S1)}$$

where σ_{ion} is the ionic conductivity, L is the film thickness, R is the resistance and A is the area. The thickness of the film is around 0.6 mm as determined by a micrometer.

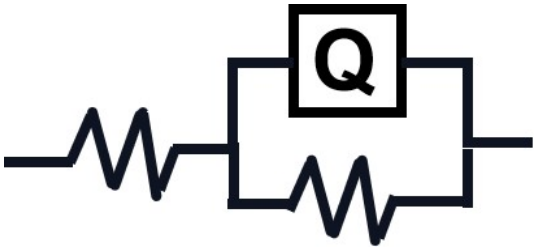

Scheme S1. Equivalent circuit for the analysis of the Nyquist plots.

The ionic Seebeck coefficients of the ionogels were measured using a home-made system as shown in **Scheme S2a**. Two open-circuit voltages were recorded for different temperature gradients. All the ionogels exhibited positive Seebeck coefficients under ambient conditions. Under a temperature gradient of 3.0 K, a consistent thermal voltage distribution was observed, with the thermal voltage peaking. The Seebeck coefficient was determined using the following equation:

$$S_i = \frac{\Delta V d_2}{\Delta T d_1} \quad \text{(S2)}$$

where ΔU is the open-circuit voltage and ΔT is the temperature difference measured by the thermocouples. The dimensions of the glass substrates were 2 × 7.5 cm^2. Copper electrodes were prepared by taping them directly onto a glass substrate using a copper

tape and then carefully patterning them with a sharp knife. The length of the copper electrodes was 2 cm and the width was approximately 0.1 cm. The distance (d_1) between the two copper electrodes was 4 cm, and the distance (d_2) between the two thermocouples was 4 cm. Before testing, the surface of the copper tape was sandpapered to remove the oxide layer. The electrodes were connected to an electrochemical workstation using alligator clips (flat opening).

The effectiveness of the ionic Seebeck coefficient device was verified by measuring the ionic Seebeck coefficient of a poly(sodium 4-styrenesulfonate) (PSSNa) film (**Scheme S2b)**. The film material consisted of 2 wt. % aqueous solution of PSSNa drop-cast on a transparent glass substrate, for which the ionic Seebeck coefficient measured at 90% relative humidity was 2.995 mVK^{-1}, which is consistent with the literature,[1] and indicates that the ionic Seebeck coefficient test device is effective and the test results are accurate. All the measurements of the thermoelectric properties were carried out near room temperature (25 ºC) and a relative humidity (RH) of 40%.

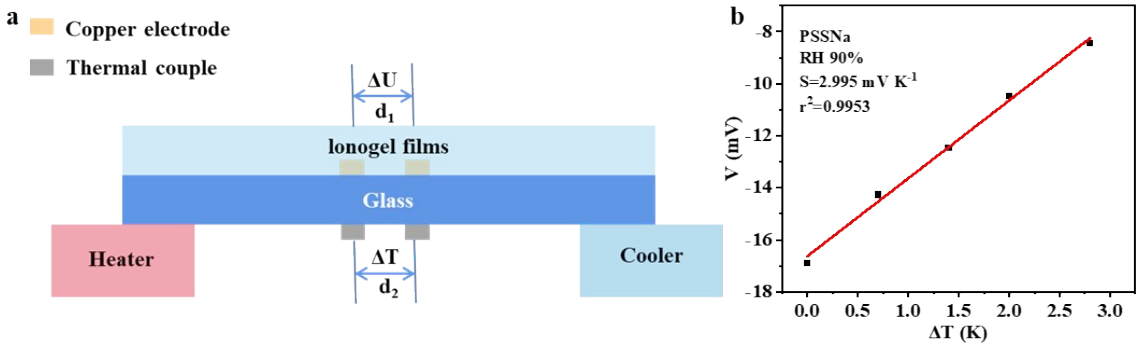

Scheme S2. a) Illustration of the configuration for Seebeck measurement. b) Linear fitting of PSSNa ionic Seebeck coefficient.

Mechanical performance test: The mechanical properties of the ionogel were measured on a WDW-0.5 microcomputer-controlled electronic universal testing machine, and the size of the ionogel to be tested was 40 mm in length, 5 mm in width, and approximately 0.6 mm in thickness, and it was tested at a tensile speed of 50 mm/min.

Characterization of other properties (UV-visible transmittance spectra, Fourier transform infrared spectroscopy (FT-IR), thermogravimetric analysis (TG), and X-ray diffraction (XRD): UV-visible transmittance spectra were acquired using a Shimadzu UV-2550 spectrophotometer. Fourier transform infrared spectra (FRIR) were scanned on an infrared spectrometer, FTIR-650, against a background of potassium bromide and using the diffuse reflectance method in the scanning range 500–4000 cm^{-1}. G analysis of the ionogels was carried out using a Discovery-TGA-550 analyzer with a nitrogen atmosphere maintained at all times during the testing process, and the temperature range of the test was 30–750 °C with a temperature increase rate of 20 °C min^{-1}. XRD spectra were obtained using a Rigaku SmartLab XRD system with a scanning range of $2\theta = 10^{o}$ to 80^{o}. Thickness was determined using an IP65 Mitutoyo micrometer.

Supplementary results

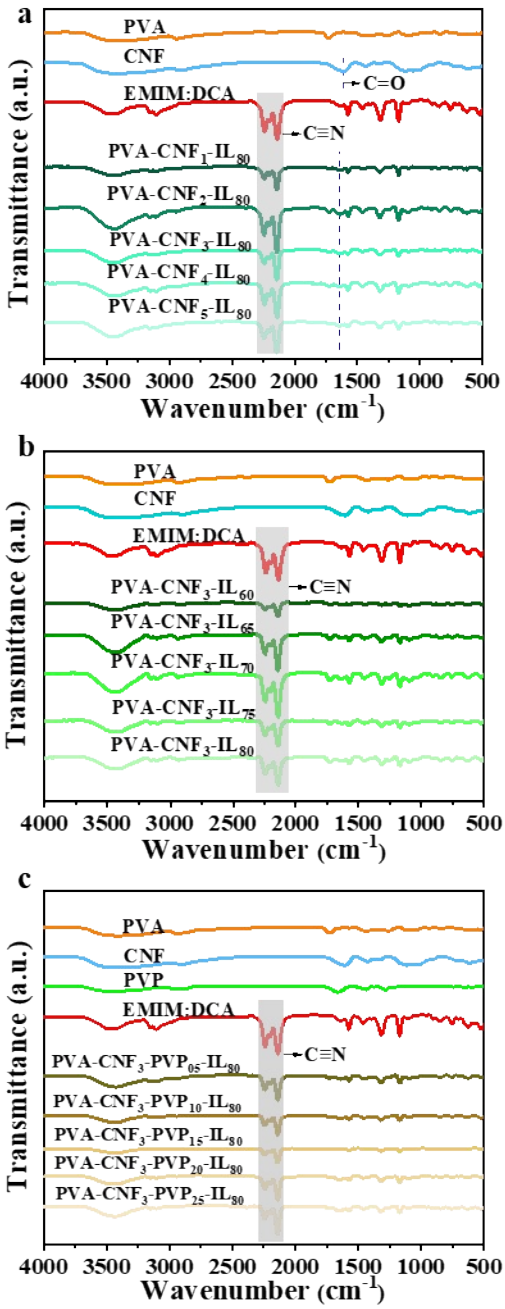

Figure S1. FTIR spectra analysis. a) PVA-CNF_x-IL_{80} ionogel. b) PVA-CNF_3-IL_n ionogel. c) PVA-CNF_3-PVP_m-IL_{80} ionogel.

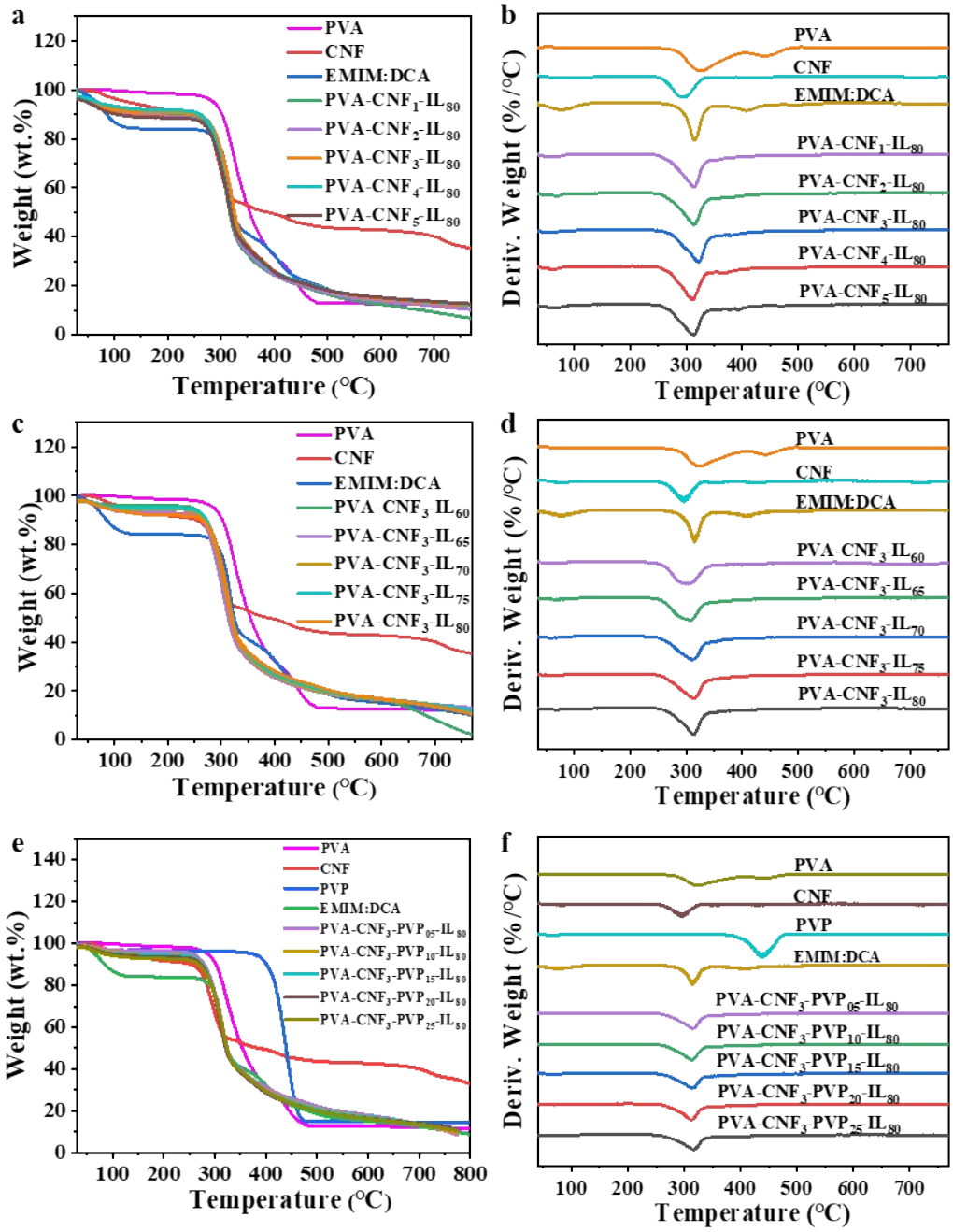

Figure S2. Thermogravimetric curve (TG) and Thermogravimetric analysis (TGA) curves. a–b) TG and DTG of PVA-CNF_x-IL_{80} ionogel. c–d) TG and DTG of PVA-CNF_3-IL_n ionogel. e–f) TG and DTG of PVA-CNF_3-PVP_m-IL_{80} ionogel.

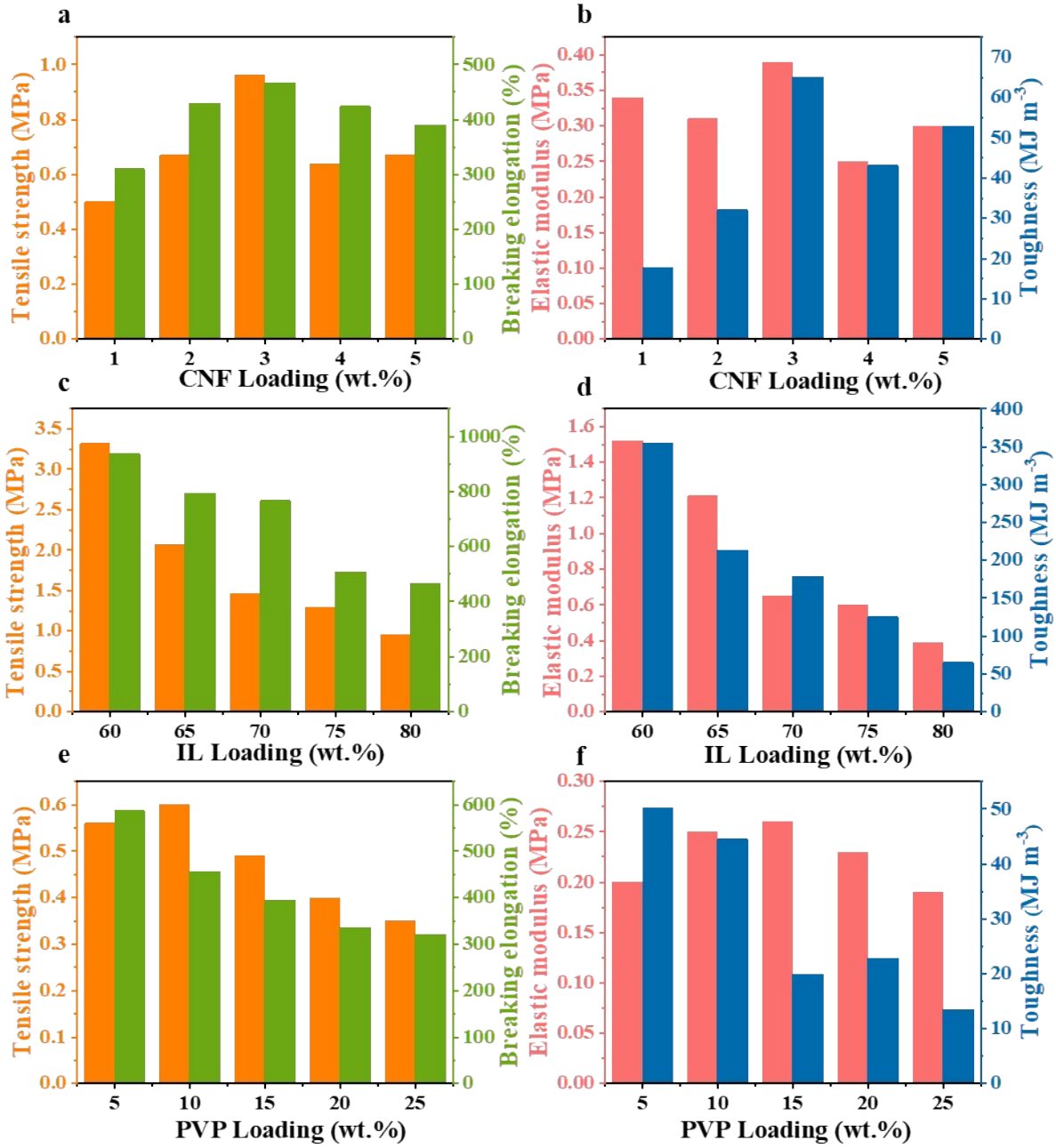

Figure S3. Mechanical properties test. a) tensile strength and elongation at break, b) elastic modulus and toughness of PVA-CNF_x-IL_{80} ionogel, c) tensile strength and elongation at break, d) elastic modulus and toughness of PVA-CNF_3-IL_n ionogel, e) tensile strength and elongation at break, f) elastic modulus and toughness of PVA-CNF_3-PVP_m-IL_{80} ionogel.

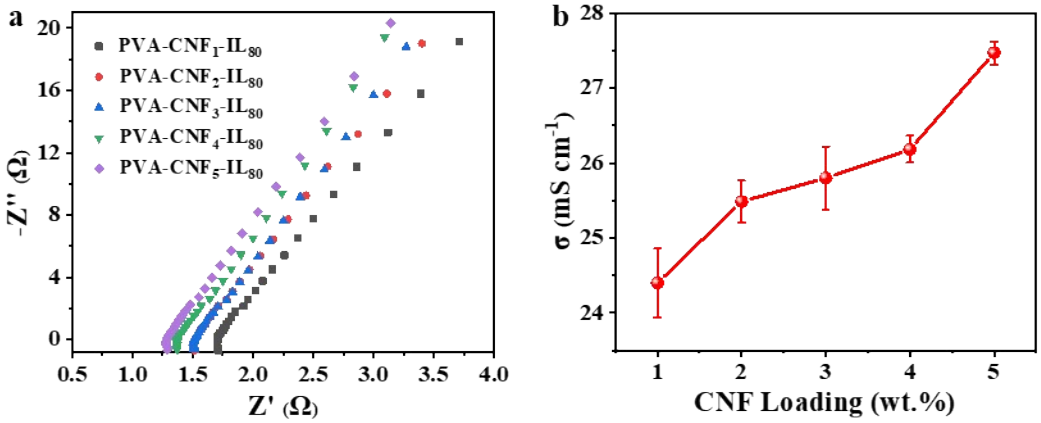

Figure S4. Ionic conductivity test of PVA-CNF_x-IL_{80} ionogels. a) Nyquist plots of PVA-CNF_x-IL_{80} ionogels with different CNF loadings. b) Ionic conductivity of PVA-CNF_x-IL_{80} ionogel with different CNF loadings.

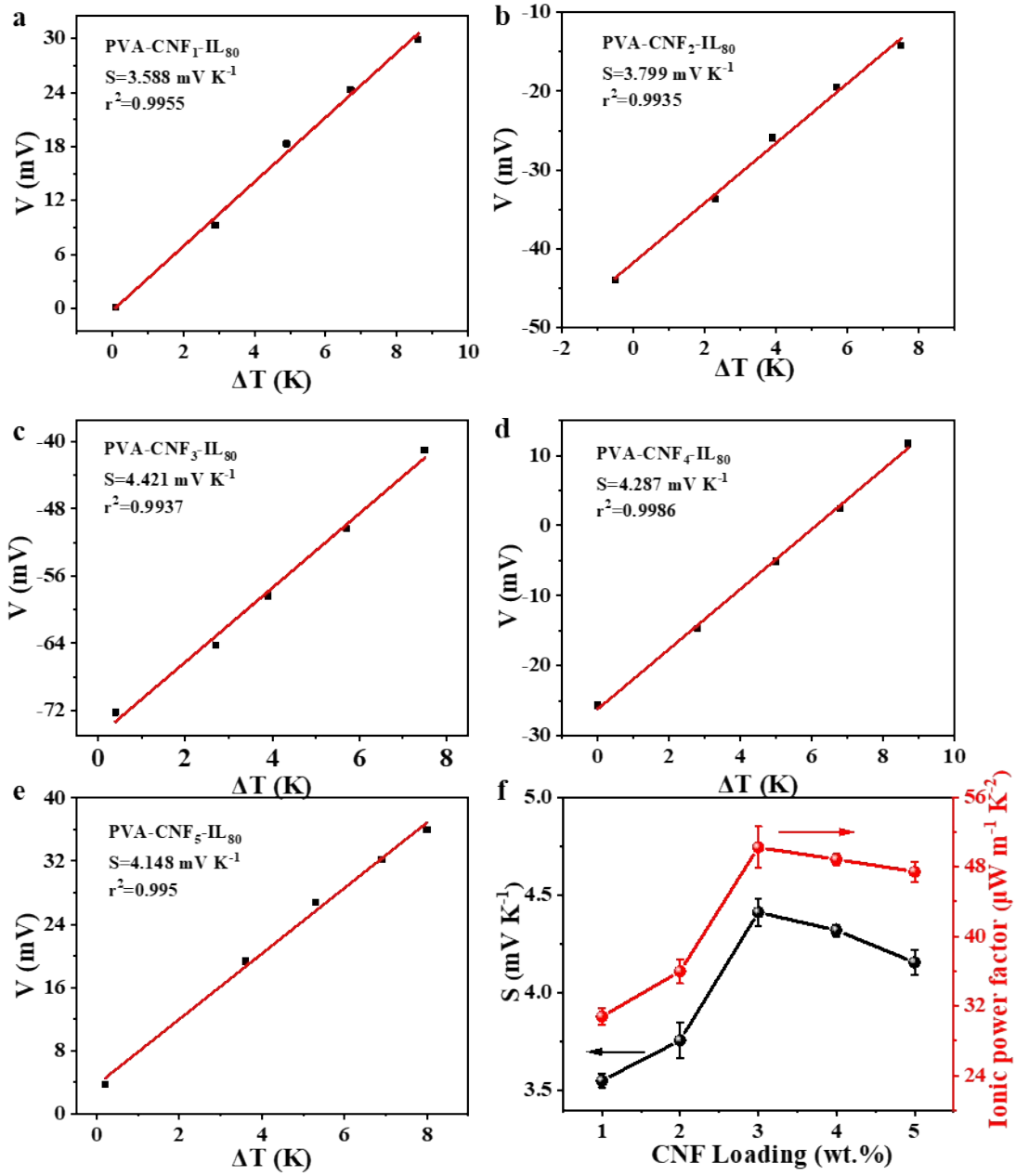

Figure S5. Ionic Seebeck coefficient test of PVA-CNF_x-IL_{80} ionogels. a-e) PVA-CNF_x-IL_{80} ionogel linear fit of ionic Seebeck coefficients, f) ionic Seebeck coefficients versus power factor with different CNF loadings.

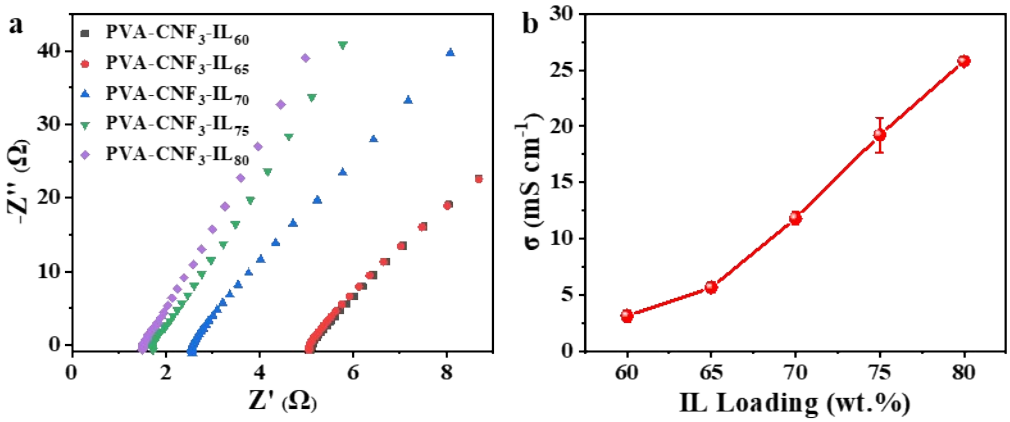

Figure S6. Ionic conductivity test of PVA-CNF_3-IL_n ionogels. a) Nyquist plots of PVA-CNF_3-IL_n ionogels with different IL loadings. (b) Ionic conductivity of PVA-CNF_3-IL_n ionogel with different IL loadings.

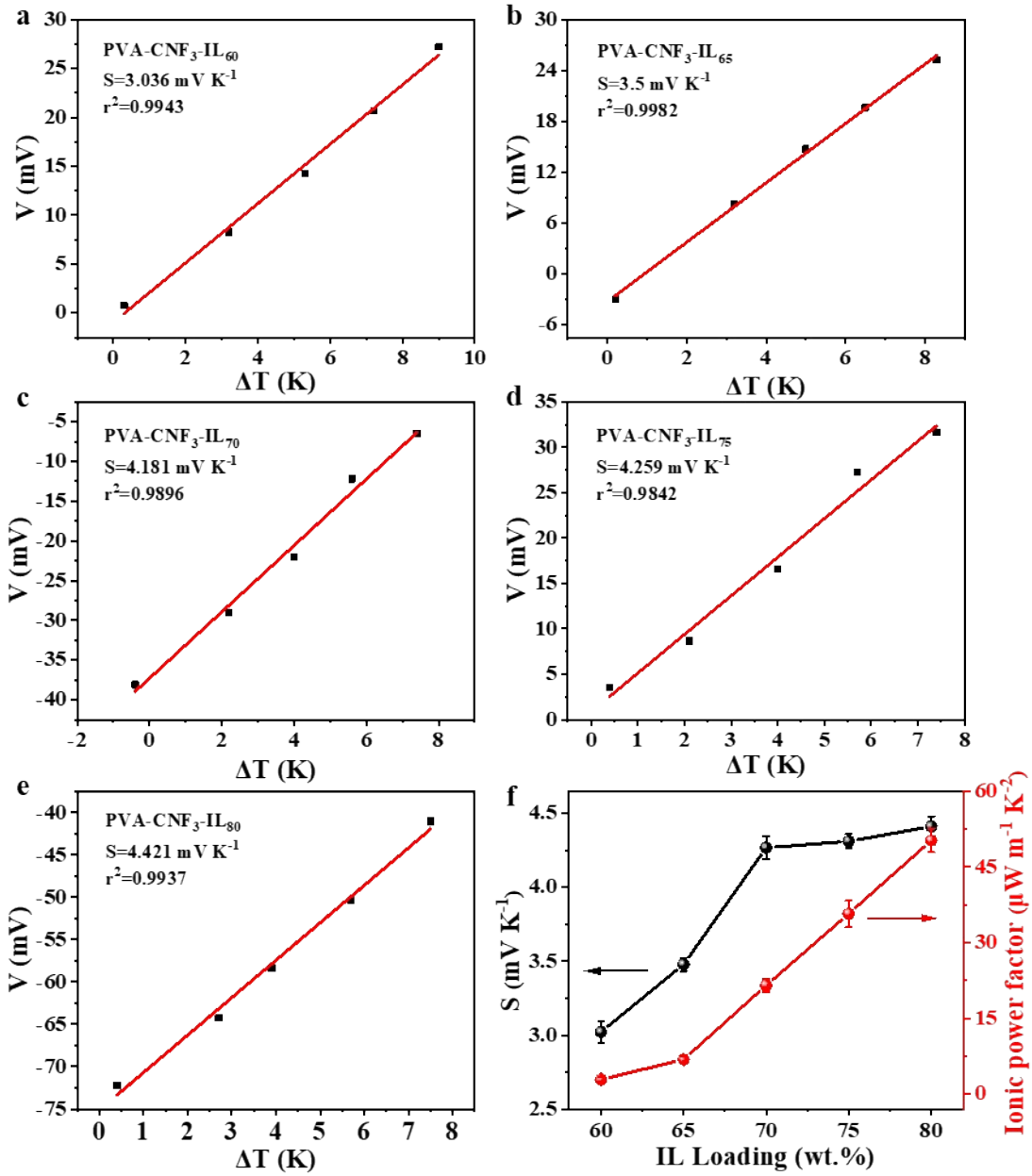

Figure S7. Ionic Seebeck coefficient test of PVA-CNF_3-IL_n ionogels. a–e) PVA-CNF_3-IL_n ionogel linear fit of ionic Seebeck coefficients, f) ionic Seebeck coefficients versus power factor with different IL loadings.

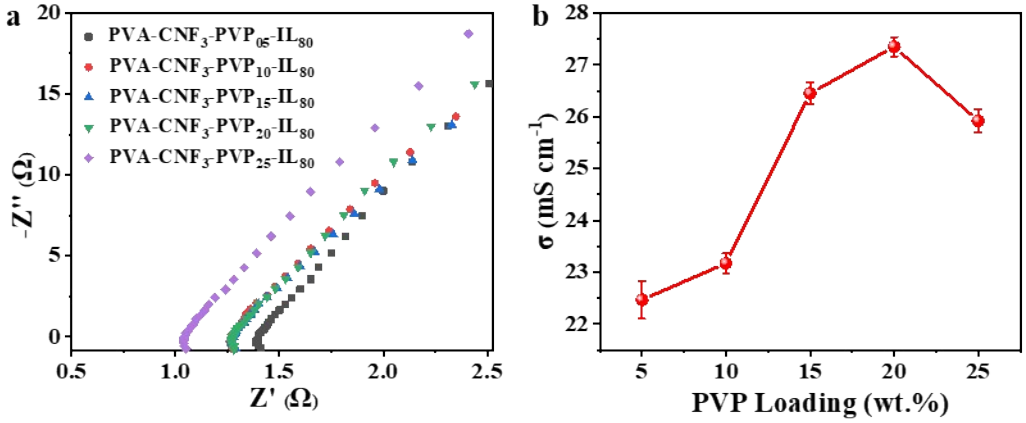

Figure S8. Ionic conductivity test of PVA-CNF_3-PVP_m-IL_{80} ionogels. a) Nyquist plots of PVA-CNF_3-PVP_m-IL_{80} ionogels with different PVP loadings. b) Ionic conductivity of PVA-CNF_3-PVP_m-IL_{80} ionogel with different PVP loadings.

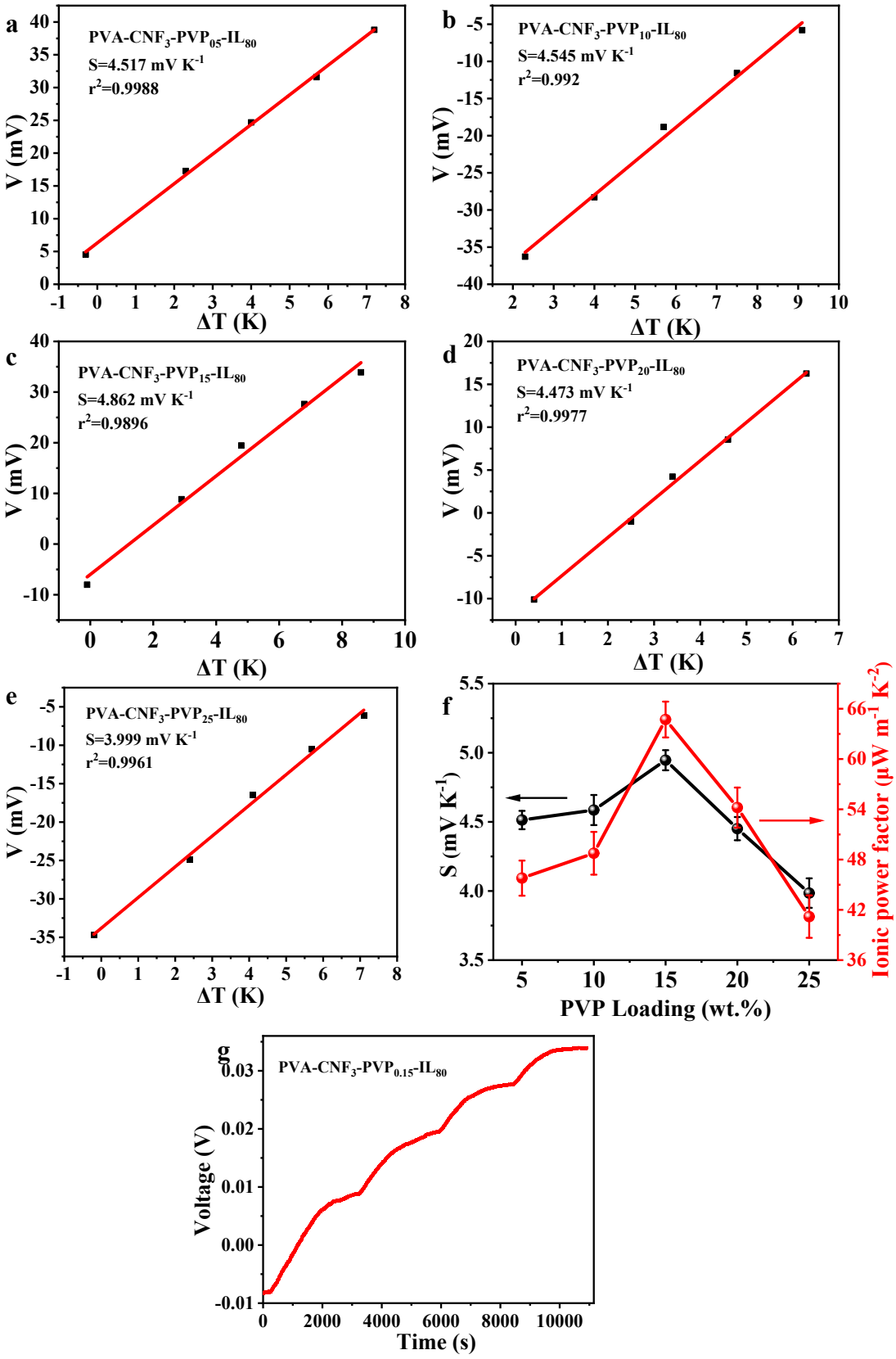
a
PVA-CNF3-PVP05-IL80
S=4.517 mV K-1
r2=0.9988
V (mV)
ΔT (K)
b
PVA-CNF3-PVP10-IL80
S=4.545 mV K-1
r2=0.992
V (mV)
ΔT (K)
c
PVA-CNF3-PVP15-IL80
S=4.862 mV K-1
r2=0.9896
V (mV)
ΔT (K)
d
PVA-CNF3-PVP20-IL80
S=4.473 mV K-1
r2=0.9977
V (mV)
ΔT (K)
e
PVA-CNF3-PVP25-IL80
S=3.999 mV K-1
r2=0.9961
V (mV)
ΔT (K)
f
S (mV K-1)
Ionic power factor (μW m-1 K-2)
PVP Loading (wt.%)
g
PVA-CNF3-PVP0.15-IL80
Voltage (V)
Time (s)

Figure S9. Ionic Seebeck coefficient test of PVA-CNF_3-PVP_m-IL_{80} ionogels. a–e) PVA-CNF_3-PVP_m-IL_{80} ionogel linear fit of ionic Seebeck coefficients, f) ionic Seebeck coefficients versus power factor with different PVP loadings, g) Voltage-time curves of PVA-CNF_3-$PVP_{0.15}$-IL_{80} thermoelectric ionogel.

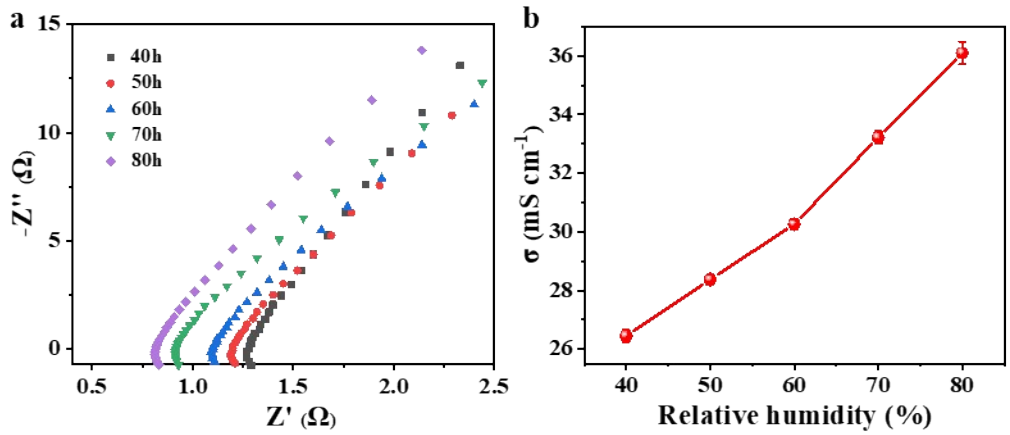

Figure S10. Ionic conductivity test of PVA-CNF_3-PVP_{15}-IL_{80} ionogels under different humidity conditions. a) Nyquist plots, b) ionic conductivity of PVA-CNF_3-PVP_{15}-IL_{80} ionogels.

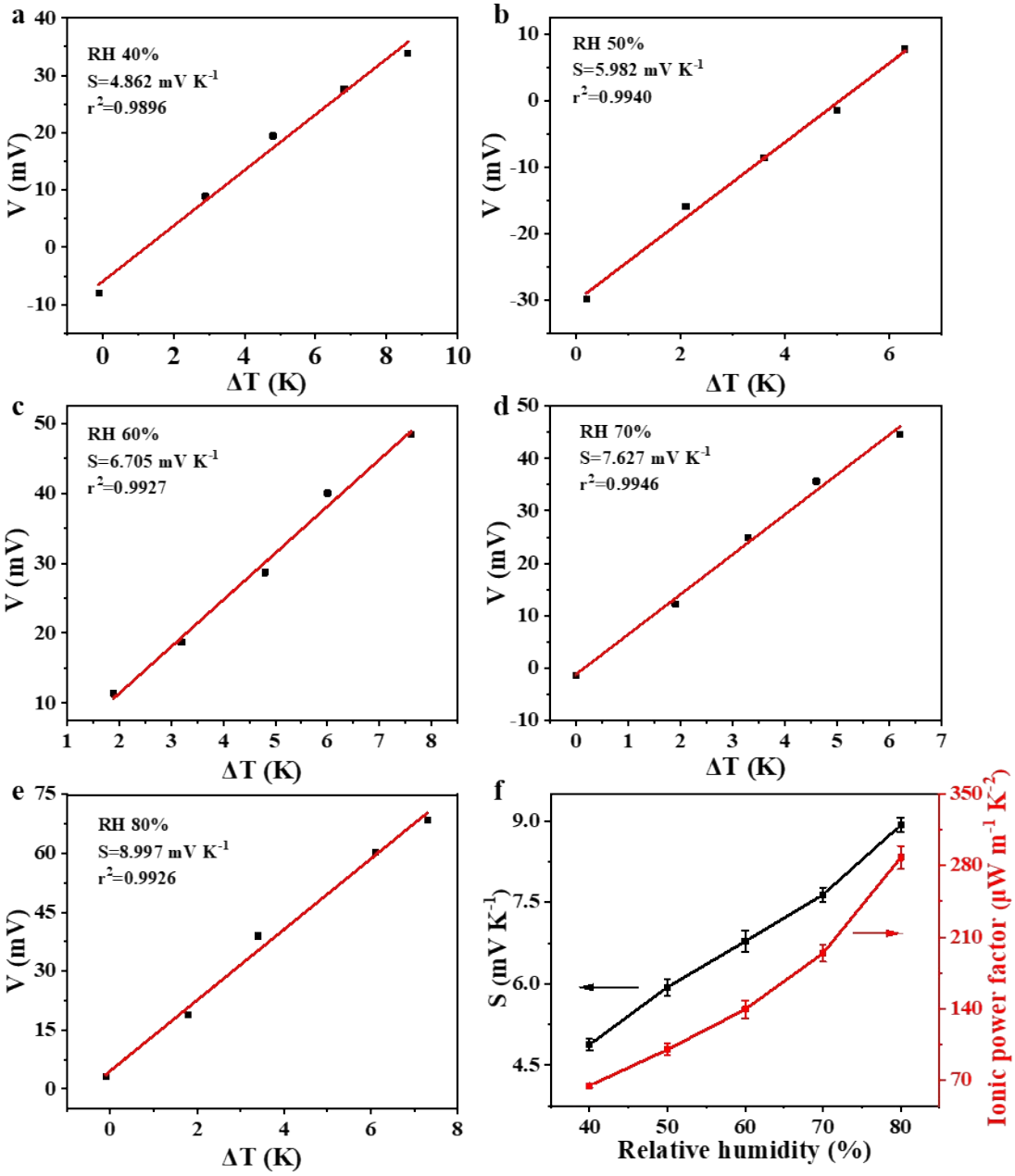

Figure S11. Ionic Seebeck coefficient test of PVA-CNF_3-PVP_{15}-IL_{80} ionogels under different humidity conditions. a–e) PVA-CNF_3-PVP_{15}-IL_{80} ionogel linear fit of ionic Seebeck coefficients, f) Ionic Seebeck coefficient and power factor versus Relative humidity.

.

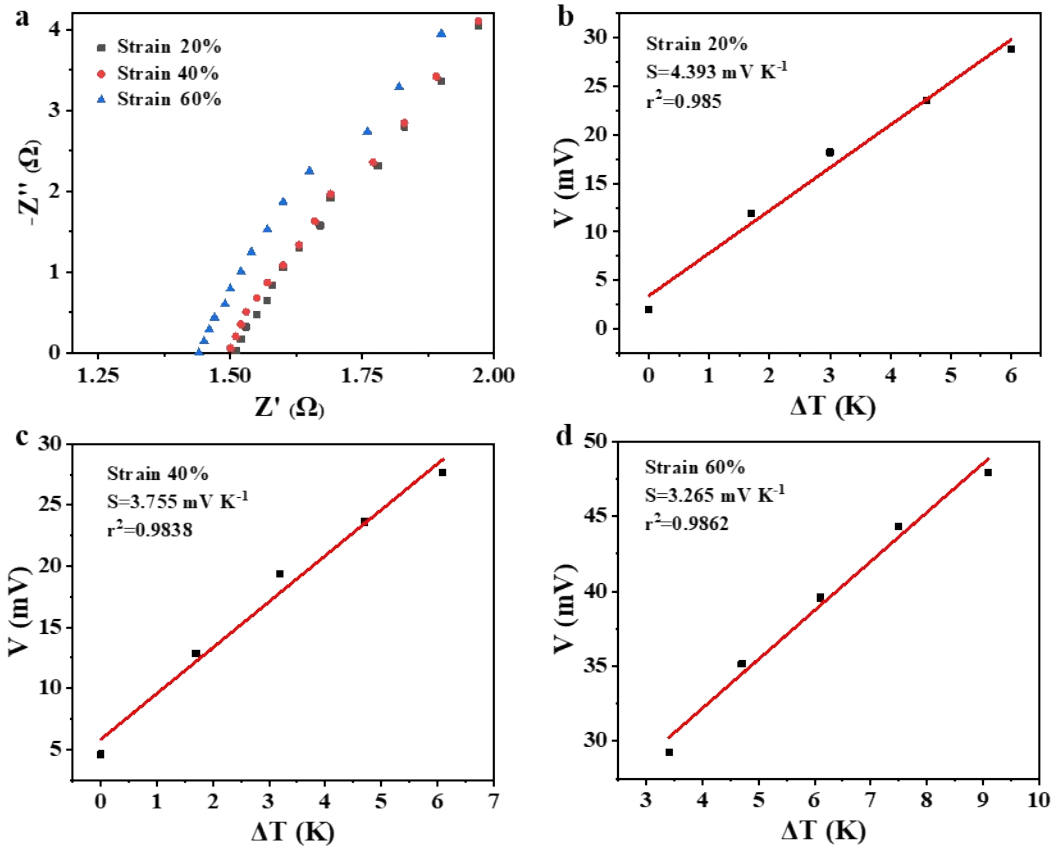

Figure S12. Thermoelectric performance test of PVA-CNF_3-PVP_{15}-IL_{80} ionogels at different strains. a) Nyquist plots of PVA-CNF_3-PVP_{15}-IL_{80} ionogels at different strains. b–d) Linear fitting of PVA-CNF_3-PVP_{15}-IL_{80} ionogel ionic Seebeck coefficient

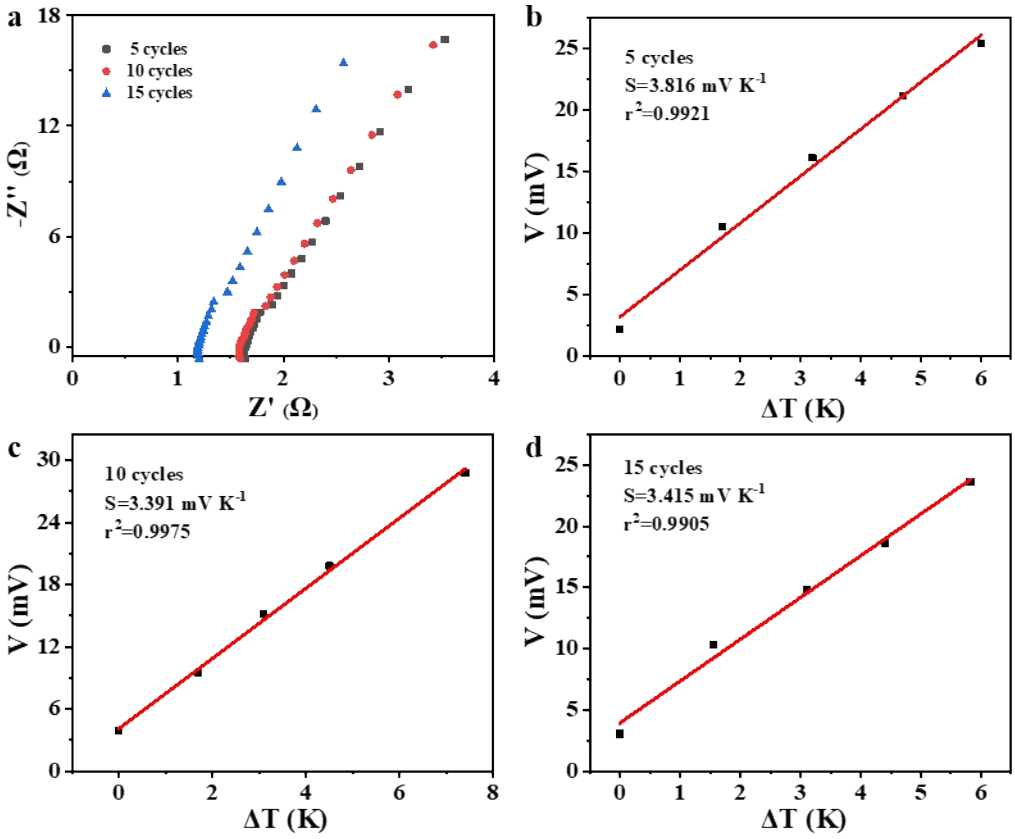

Figure S13. Thermoelectric performance test of PVA-CNF_3-PVP_{15}-IL_{80} ionogels for 40% stretch/release cycles.. a) Nyquist plots of PVA-CNF_3-PVP_{15}-IL_{80} ionogels for 40% stretch/release cycles. b–d) Linear fitting of PVA-CNF_3-PVP_{15}-IL_{80} ionogel ionic Seebeck coefficient.

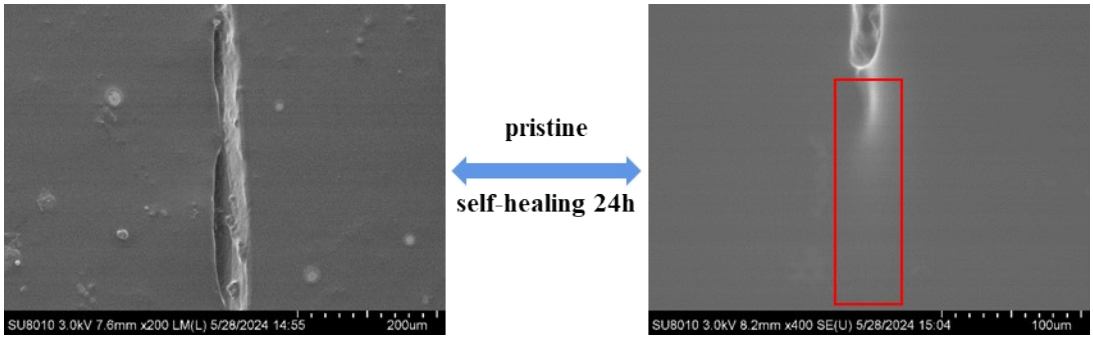

Figure S14. The SEM images before and after self-healing.

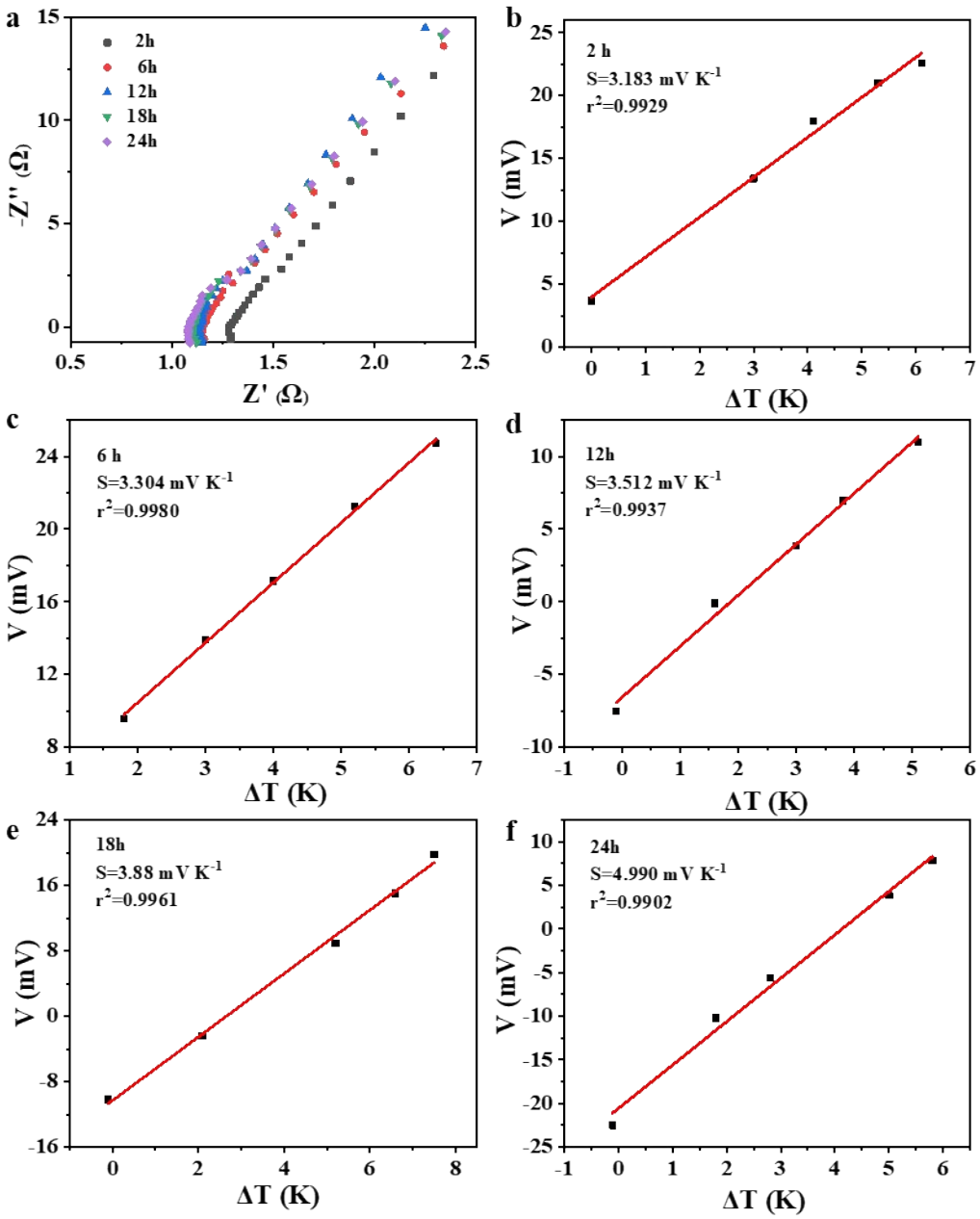

Figure S15. Thermoelectric performance test of PVA-CNF_3-PVP_{15}-IL_{80} ionogels with different self-healing times. a) Nyquist plots of PVA-CNF_3-PVP_{15}-IL_{80} ionogels with different self-healing times. b–f) Linear fitting of PVA-CNF_3-PVP_{15}-IL_{80} ionogel ionic Seebeck coefficient with different self-healing times.

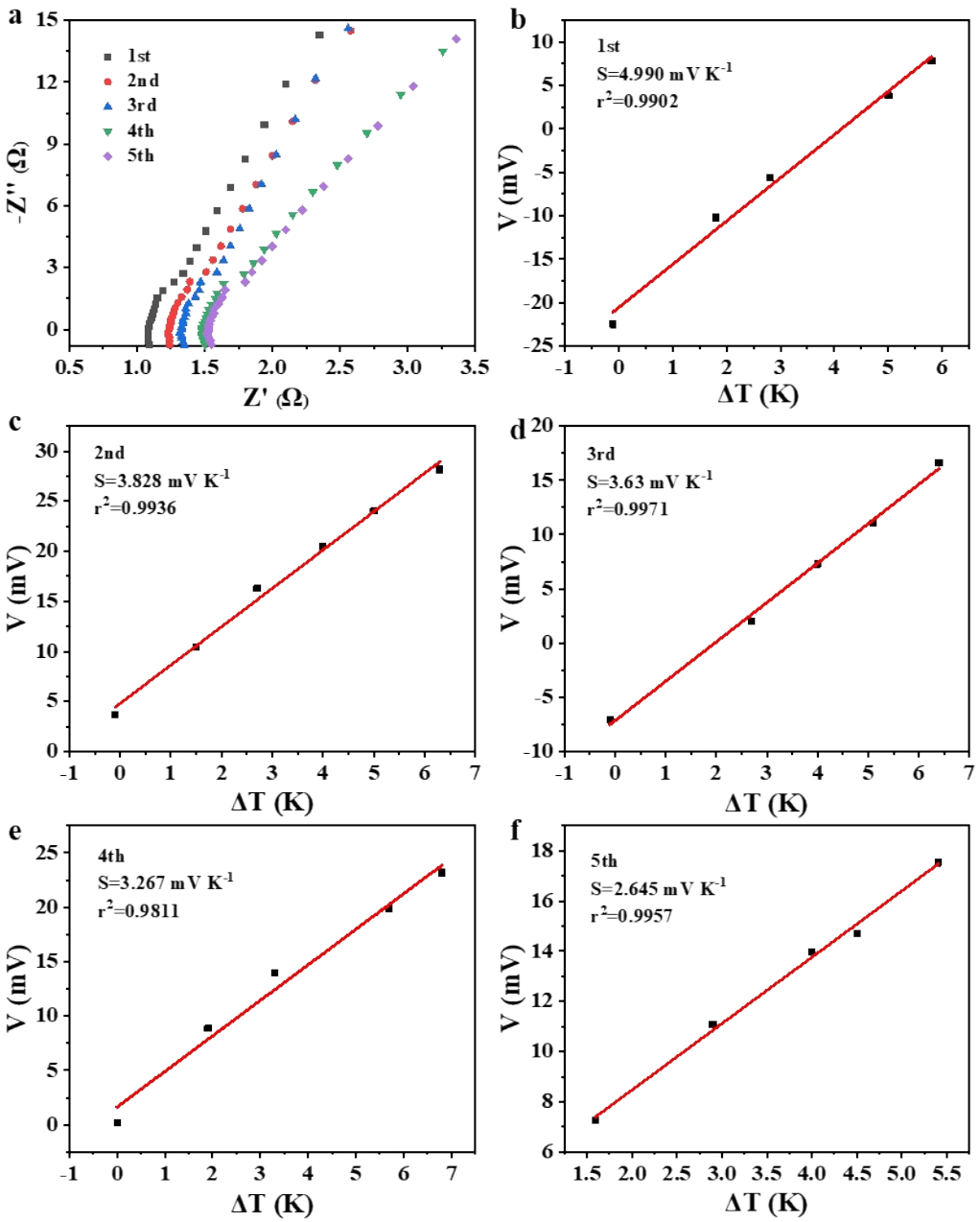

Figure S16. Thermoelectric performance test of PVA-CNF_3-PVP_{15}-IL_{80} ionogels with different self-healing cycles. a) Nyquist plots of PVA-CNF_3-PVP_{15}-IL_{80} ionogels with different self-healing cycles. b–f) Linear fitting of PVA-CNF_3-PVP_{15}-IL_{80} ionogel ionic Seebeck coefficient with different self-healing cycles.

Figure S17. Mechanical properties of ionogels with different times of self-healing. a) tensile strength and elongation at break of PVA-CNF_3-PVP_{15}-IL_{80} ionogel, b) elastic modulus and toughness of PVA-CNF_3-PVP_{15}-IL_{80} ionogel.

References

1 H. Wang, D. Zhao, Z. U. Khan, S. Puzinas, M. P. Jonsson, M. Berggren, X. Crispin. *Adv. Electron. Mater.*, 2017, **3**, 1700013.